CONFIDENTIAL

Copy /
RM SL52K05



NACA

# RESEARCH MEMORANDUM

for the

Bureau of Ordnance, Department of the Navy

## A WIND-TUNNEL INVESTIGATION OF THE STABILITY OF THE ANTISUBMARINE ROCKET MK 1 MOD 0

By Jacob H. Lichtenstein and James L. Williams

Langley Aeronautical Laboratory
Langley Field, Va.



NATIONAL ADVISORY COMMITTEE
FOR AERONAUTICS

WASHINGTON

NOV 13 1952



CONFIDENTIAL

NATIONAL ADVISORY COMMITTEE FOR AERONAUTICS

RESEARCH MEMORANDUM

for the

Bureau of Ordnance, Department of the Navy

# A WIND-TUNNEL INVESTIGATION OF THE STABILITY OF THE ANTISUBMARINE ROCKET MK 1 MOD 0

By Jacob H. Lichtenstein and James L. Williams

## SUMMARY

An investigation has been made in the Langley stability tunnel in an attempt to determine the cause and a remedy for the instability in flight of the Bureau of Ordnance, Department of the Navy; antisubmarine rocket Mk 1 Mod 0.

The results of the investigation indicate that the Magnus effects and their nonlinear variation with angle of attack are important factors in the stability of this missile. Reversing the direction of rotation of the arming propeller such that the propeller and body rotated in the same direction decreased the Magnus effects and it is believed that an increase in size or resisting torque of the reversed propeller would further decrease the Magnus effects. A nose-ring spoiler combined with rotation of the propeller in the original direction (opposite to the body rotation) appeared to be the most promising configuration in that the Magnus effects were smallest. The nose-ring spoiler, however, caused an increase in drag of about 10 to 12 pounds, full scale.

## INTRODUCTION

The Bureau of Ordnance, Department of the Navy, has recently developed an antisubmarine rocket designated as the Mk 1 Mod 0. This missile is projected through the air from a ship to a point on the water surface above a suspected submarine location where it descends to the proper depth and is discharged. Both spin and fin stabilization is employed during the flight of the missile and its maximum range is about 800 yards.

During firing tests made for the purpose of preparing range tables, the missile exhibited undesirable stability characteristics for certain combinations of azimuth launching angle and side-wind velocity. As each round emerges from the launching tube, the effects of gravity and side

wind cause the missile axis to assume an angle of attack. The longitudinal stability of the missile tends to reduce this angle. However, the pitching moment in combination with the spin of the missile introduces a gyroscopic moment that causes the longitudinal axis of the missile to precess around the flight-path axis. A satisfactory flight is considered one in which the angle between the missile axis and flight path is about $10^\circ$ or less. When the missile is launched at relative bearings of $65^\circ$ to $135^\circ$ measured from the bow of a ship traveling at 33 knots, the angular deviation between the missile axes and the flight path becomes excessively large (about $30^\circ$). This results in increased dispersion of the rounds and may also cause destruction of the round upon contact with the water, reference 1.

As a result of the instability of this missile, a wind-tunnel investigation was made in the Langley stability tunnel at the request of the Bureau of Ordnance, Department of the Navy, in order to determine, if possible, the cause and a remedy for this condition. The results of this investigation are summarized in this paper.

This investigation included tests on both a stationary and a rotating model in order to assess the importance of the aerodynamic forces associated with spin (Magnus effects) on the stability of the missile. In addition, the stability-tunnel rolling flow facilities were employed for a portion of the tests in order to determine the aerodynamic resistance to the precessional motion observed in flight. The influence of a turbulence-creating ring around the nose of the missile and the influence of the direction of rotation of the arming propeller on the stability of the missile were also determined.

## SYMBOLS

The data presented herein are in the form of standard NACA coefficients of forces and moments which are referred to the wind or flight axes, with the origin at the assumed center of gravity of the missile. The positive direction of the forces, moments, angles, and angular velocities are shown in figure 1. The coefficients and symbols are defined as follows:

$C_L$ lift coefficient, $L/qS$

$C_D$ drag coefficient, $D/qS$

$C_Y$ side-force coefficient, $Y/qS$

$C_m$ pitching-moment coefficient, $M/qSl$

$C_n$ yawing-moment coefficient, $N/qSl$

$C_l$ rolling-moment coefficient $L'/qSl$

L lift, lb

D drag, lb

Y side force, lb

M pitching moment about assumed center of gravity, ft-lb

N yawing moment, ft-lb

L' rolling moment, ft-lb

q dynamic pressure, $\frac{1}{2}\rho V^2$, lb/sq ft

$\rho$ mass density of air, slugs/cu ft

V velocity, ft/sec

S maximum cross-sectional area, sq ft

$l$ fuselage length, ft

d maximum diameter of fuselage, ft

$\alpha$ angle of attack, deg

p rate of roll about wind axis, precessional velocity, radians/sec

$\frac{pd}{2V}$ rolling-velocity parameter

$\omega$ rate of rotation about longitudinal axis of model, rpm

$\Omega$ rate of rotation of propeller, rpm

$$C_{l_p} = \frac{\partial C_l}{\partial \frac{pd}{2V}}$$

$$C_{n_p} = \frac{\partial C_n}{\partial \frac{pd}{2V}}$$

$$C_{Y_p} = \frac{\partial C_Y}{\partial \frac{pd}{2V}}$$

$C_{l_T}$, $C_{n_T}$ total rolling and yawing moments for the spinning missile (for example, $C_{l_T} = C_l + C_{l_p} \frac{pd}{2V}$)

## APPARATUS, MODELS, AND TESTS

The tests of this investigation were made in the 6-foot circular test section of the Langley stability tunnel. This section is equipped with a motor-driven rotor which may be employed to impart a twist to the air stream so that the model mounted rigidly in the tunnel is in a field of flow similar to that which exists in rolling flight (ref. 2).

The models used in the present investigation were 1/2-scale models of the Bureau of Ordnance, Department of the Navy, antisubmarine rocket Mk 1 Mod 0. A sketch showing the general arrangement of the models is presented in figure 2. The body of the stationary model was made of solid pine with a cut-out for mounting. The tail was made of sheet metal. The tail fins within the shroud were canted with the leading edge 7° to the right of the missile longitudinal axis as seen in a plan view. The rotating model was constructed entirely of mahogany. In order to attach the rotating model to the support system it was necessary to hold a portion of the model stationary. This stationary section, which was 13 inches long, contained the driving motor and bearings for the shaft that rotated the forward and rearward rotating sections. (See fig. 2.) Since the shaft had to be along the center line it was necessary to attach the model to the support system 1 inch below the assumed center of gravity. In order to minimize the effects of flow through the gap between the stationary and rotating sections a 1-inch-wide band of aluminum was attached to the stationary section so that it overlapped the gap about 1/2 inch on each side. (See figs. 2 and 3.) Because of a time limitation during the model construction it was necessary to compromise the desired rotational speed of the model for a simple drive system. The design, as used, allowed the model to rotate freely under the aerodynamic force of the fins. The motor installed in the model had only sufficient power to rotate the model at about 300 rpm and was installed with a slip clutch so that it drove the model only when the rotational speed dropped to around 300 rpm. The model rotated in a clockwise direction as seen from the rear and the rotational speeds through the angle-of-attack range for the various configurations are presented in table I. Two arming propellers were tested; one propeller rotated as on the full-scale missile; in the opposite direction to that

of the model (counterclockwise), whereas the other propeller tested rotated in the same direction as the model (clockwise). The propeller shafts and blades were made of steel and the housing was made of aluminum. The shaft was mounted in ball bearings so that it was freely rotating, and no torque other than the bearing friction was applied. Measurement of this bearing friction indicated a resisting torque of about 0.1 inch-ounce. The spoiler-nose ring was a 1/16-inch-diameter welding rod formed in a circle of $6\frac{3}{8}$ inches outside diameter and was attached around the nose of the model at the location shown in figure 2. The models were mounted on a single-strut support which was attached to a conventional six-component balance system. Photographs of the rotating model mounted in the Langley stability tunnel are presented in figure 3.

The tests were made at a dynamic pressure of 39.7 pounds per square foot which corresponds to a Mach number of 0.17 and a Reynolds number of $4.84 \times 10^6$ based upon the model length. The model was tested through an angle-of-attack range from about $-4^\circ$ to about $40^\circ$ at zero sideslip in both straight and rolling flow with the model stationary and rotating. The tests were made with and without a nose ring for the propeller-off, counterclockwise-propeller, and clockwise-propeller configurations. In addition, some brief tests were made with the tail fins and shroud extended about 50 percent of their original length.

## CORRECTIONS

Corrections were applied to the lift, drag, and pitching moment for the support-strut tares. The moment data for the rotating model have been transferred from the mounting point to the assumed center-of-gravity location. No corrections were applied for blockage or jet-boundary effects inasmuch as they were found to be of negligible magnitude. Corrections for the interference of the support strut and stationary section of the spinning missile were not applied to the lateral coefficients because means for their evaluation was not readily apparent.

## RESULTS AND DISCUSSION

### Presentation of Data

The straight-flow data for the rotating model without and with a nose ring are presented in figures 4 and 5, respectively, and for the stationary model without and with the nose ring in figures 6 and 7, respectively. The rolling-flow data for the rotating model without and with the nose ring are presented in figures 8 and 9, respectively, and

for the available configurations of the stationary model without the nose ring in figure 10. The total rolling moment and yawing moment are presented in figures 11 and 12, respectively, for the rotating model without and with the nose ring. The model rotational speed $\omega$ through the angle-of-attack range for various configurations is presented in table I. The propeller rotational speed $\Omega$ is also presented in table I. Typical values are given because changes in $\Omega$ with changes in model configuration were insignificant magnitude.

## Longitudinal Characteristics

The curves of lift, drag, and pitching moment against angle of attack (figs. 4, 5, 6, and 7) show that, other than a general increase in drag due to the nose ring, the nose ring and direction of propeller rotation had little influence on the longitudinal parameters as could be expected. These factors, if generally linear as shown here, should not be a primary contribution to an instability of the type reported for this missile. The data show that the increment in drag due to addition of the nose ring was larger on the stationary model than on the rotating model.

## Lateral Characteristics

Straight flow.- The lateral force and moment coefficients $C_Y$, $C_l$, and $C_n$ for a body with no spin and perfect symmetry of flow should be about zero. Development of an asymmetrical wake due to instability of a symmetrical wake or by the influence of rotation of the body or its components results in a deviation of these coefficients from zero. The forces and moments which arise due to circulation when the missile is rotating at an angle of attack are called the Magnus effects. These forces and moments are usually destabilizing (ref. 3) in that they feed energy into the precessional motion of the missile. If these Magnus effects are sufficiently large, a precession of increasing amplitude results. It appears therefore that it would, in general, be good to maintain these forces and moments small and preferably zero.

Inasmuch as the model was allowed to spin freely under the aerodynamic influence of the fins, the rate of spin varied with angle of attack (table I) and the scale spin necessary for the same value of $\frac{\omega d}{2V}$ on the model and full-scale missile was not faithfully reproduced. For most of the angle-of-attack range the model rate of spin was higher than the required scale spin (about 480 rpm). Because of this condition and the fact that no corrections for the interference of the support strut and stationary section of the rotating model were applied to these parameters, the values are not quite representative of full-scale values. The variation with angle of attack for these parameters, however, and their approximate magnitude are indicated.

The data presented in figure 4 for the rotating model show that the forces and moments vary nonlinearly with angle of attack for all the configurations. The values were small at the low angles of attack and increased rapidly beyond $\alpha = 8^\circ$ to a maximum at about $\alpha = 16^\circ$. The small values at the low angles of attack are about the magnitude of reliable measurement. Removing the propeller provided very little improvement; however, reversing the direction of propeller rotation provided considerable improvement in that the increase in the Magnus effects was delayed until higher angles of attack were obtained and the magnitudes of these effects were generally decreased. It should be noted that changing the direction of propeller rotation affected the rate of spin of the model (going from the counterclockwise to the clockwise propeller rotation decreased the model rate of spin). The effects of the propeller on the lateral-stability parameters therefore are due in part to the direct effect of the propeller on the flow and in part to the indirect effect of the propeller in changing the rate of spin. The fact that the Magnus force obtained for all the propeller configurations is negative whereas the moments are positive indicates that the center of pressure is rearward of the center of gravity. At an angle of attack of $16^\circ$ the indications are that the center of pressure would be about 3 feet, full scale, rearward of the center of gravity.

With the nose ring installed (fig. 5) the magnitude and variation of the forces and moments were considerably smaller than for the nose-ring-off configurations for angles of attack up to about $20^\circ$. This is particularly noticeable for the model with counterclockwise-propeller configuration. For the configuration with the nose ring on, the effect of propeller rotation was just the opposite to the effect of propeller rotation for the configuration with the nose ring off; the clockwise propeller now was adverse. (Compare figs. 4 and 5.)

The data in table I show that the rotational velocity of the model reached a maximum usually between $\alpha = 8^\circ$ and $\alpha = 12^\circ$ then decreased with angle of attack until about $\alpha = 24^\circ$ where the rotational velocity tended to level off. For most of the angle-of-attack range the rotational velocity was higher than that which could be obtained from the motor indicating that the fins were forcing the model to rotate.

As discussed in references 4 and 5, it is possible for a missile of this type to develop a large-amplitude wobbling motion, somewhat similar to the motion described in this paper, if the spinning velocity and the normal frequency in pitch or yaw are about the same. However, for the present case, the spinning velocity is about 12 times the value of the frequency in either pitch and yaw; the instability therefore is more likely a result of the combination of aerodynamic and gyroscopic forces than the cross-coupling effects of the rolling and pitching or yawing frequencies.

The data presented in figure 6 for the stationary model without the nose ring show that, for the nearly symmetrical case (body, hub, and tail), the values of these parameters were relatively close to zero, up to about $\alpha = 20^\circ$, as would be expected. The effect of propeller rotation on the stationary model up to $\alpha = 20^\circ$ was similar in trend although different in magnitude to the propeller effects obtained on the rotating model (fig. 4). The increments in the moments due to addition of either of the two propellers to the stationary model without propeller were of comparable magnitude to the total moments measured for the rotating model configurations even though the effects of the oppositely rotating propellers were not symmetrical.

The effect of the nose ring on the stationary model was similar to its effect on the rotating model, that is, decreasing the magnitude and variation of the forces and moments with angle of attack and also reversing the effect of the propeller rotation.

Some brief tests were made with the length of the fins and shroud increased by 50 percent. Inasmuch as the tests were of an exploratory nature and the results were not significantly different than those for the original tail, the data are not presented. This result is similar to that found in reference 1 in which moderate changes in the tail configuration did not appreciably change the flight characteristics of the missile.

Rolling flow.- The information available on the behavior exhibited by this missile in free flight indicates that the motion is primarily one of precession about the flight path at a constant rate. This condition is closely simulated by the rolling-flow facility of the stability tunnel.

The results of rolling-flow tests in this facility (figs. 8, 9, and 10) show that the aerodynamic resistance arising in proportion to the precessional velocity $\left(\text{negative } C_{l_p}\right)$ increased approximately as a function of the angle of attack squared up to about $\alpha = 28^\circ$. The various modifications considered herein, that is, removing the propeller, reversing the propeller rotation, or adding a nose ring, had no appreciable effect on the values of $C_{l_p}$ up to fairly high angles of attack.

The following analysis is made to illustrate how the total aerodynamic moment would affect the behavior of this missile for the idealized case represented by the rolling-flow tests. Curves of the total rolling and yawing moment plotted against angle of attack are presented in figures 11 and 12, repectively. These total moments $C_{l_T}$ and $C_{n_T}$ are given by

$$C_{l_T} = C_l + C_{l_p} \frac{pd}{2V}$$

$$C_{n_T} = C_n + C_{n_p} \frac{pd}{2V}$$

where $C_l$, $C_n$, $C_{l_p}$, and $C_{n_p}$ are obtained from figures 4 to 10 and $\frac{pd}{2V}$ is computed using $p = \pi$ radians per second (which approximates the value given in ref. 1). As mentioned previously, inasmuch as the scale spin of the missile was not exactly duplicated, the magnitudes of the values are not quite representative of full-scale values although the variation with angle of attack should be of the proper form.

For the configuration without the nose ring and with the counterclockwise propeller, both moments increase sharply at $\alpha = 10^\circ$ indicating that these aerodynamic components are now adding energy to the system. In order to consume this excess energy and maintain equilibrium, it would be necessary for the missile to precess more rapidly and increase its angular deviation. At about $\alpha = 26^\circ$, both moments drop to about zero and equilibrium is again established. It is indicated, therefore, that equilibrium is possible below $\alpha = 10^\circ$ and at about $\alpha = 26^\circ$ which is in general agreement with actual firing (ref. 1). Reversing the direction of rotation of the propeller delayed the increase in moments until $\alpha = 14^\circ$ and also reduced the magnitude somewhat. Although this is a definite improvement, it is not a complete answer because certain combinations of azimuth launching angle and side-wind velocity could provide conditions under which the angle of deviation would become as large as $14^\circ$. The behavior of the missile then would be similar to that for the counterclockwise propeller. From these results, however, it appears that increasing the size or resisting torque of the clockwise propeller may provide a further decrease in Magnus effects.

Installing the spoiler-nose ring on the configuration with the counterclockwise propeller delayed the increase in rolling moment until about $\alpha = 24^\circ$ while the yawing moment did not become positive throughout the angle-of-attack range. It appears, therefore, that if this configuration were displaced to some moderate angle of deviation (approximately $18^\circ$ to $20^\circ$) there would be no aerodynamic force tending to drive the missile to still larger angles. The effect of the nose ring on the clockwise-propeller configuration was not as beneficial as for the ~~original~~ counterclockwise propeller since both moments increased in a positive direction at around $\alpha = 14^\circ$.

## CONCLUDING REMARKS

The results of a wind-tunnel investigation of the Bureau of Ordnance, Department of the Navy, antisubmarine rocket Mk 1 Mod 0 indicate that the Magnus effects and their nonlinear variation with angle of attack are important factors in the stability of this missile. Other researches have indicated that reducing the Magnus effects should provide an improvement in the stability of spinning missiles. Reversing the direction of the propeller rotation (propeller and missile rotating in the same direction) decreased the Magnus effects, and it is believed that increasing the size or resisting torque of the reversed propeller would further decrease the Magnus effects. The combination of nose-ring spoiler and original direction of propeller rotation (propeller and missile rotating in opposite directions) appeared to be the most promising configuration in that the Magnus effects were smallest through most of the angle-of-attack range and there was no increase in these effects until angles of attack of about 20° were attained. The nose ring caused, however, an increase in drag of about 10 to 12 pounds, full scale.

Langley Aeronautical Laboratory,
National Advisory Committee for Aeronautics,
Langley Field, Va.

Jacob H. Lichtenstein
Aeronautical Research Scientist

James L. Williams
Aeronautical Research Scientist

Approved: Thomas A. Harris

Thomas A. Harris
Chief of Stability Research Division

RSI

## REFERENCES

1. Jones, A. L.: Ballistic Calibration of Rockets and Preparation of Rocket Range Tables, Thirteenth Partial Rep. Additional Firing Tests at Sea of the 12.75" Rocket Mk 1 Mod 0, Second Partial Rep. NPG Rep. No. 875, U.S. Naval Proving Ground, Dahlgren, Va., Oct. 1, 1951.

2. MacLachlan, Robert, and Letko, William: Correlation of Two Experimental Methods of Determining the Rolling Characteristics of Unswept Wings. NACA TN 1309, 1947.

3. Anon.: The Motion of Rotated and Unrotated Rockets. Rep. No. 1943/19, British P.D.E., June 1943.

4. Phillips, William H.: Effect of Steady Rolling on Longitudinal and Directional Stability. NACA TN 1627, 1948.

5. Schneller, E.: On the Wabbling Motion of an Arrow Stable Body at Free Flight, Part I. The Mechanism of an Activated Wabbling Motion of Arrow-Stable Bodies, Part II. Translation R-30-18, Part 31, Goodyear Aircraft Corp., June 7, 1946. (From Archiv 187 and Archiv 189, July 3, 1945.)

TABLE I.- ROTATIONAL SPEEDS OF THE MODEL AND OF THE PROPELLER IN REVOLUTIONS PER MINUTE

| α | Complete model counterclockwise propeller | Complete model clockwise propeller | Body hub and tail | Complete model counterclockwise propeller plus nose ring | Complete model clockwise propeller plus nose ring | Body, hub, and tail plus nose ring | Propeller |
|---|---|---|---|---|---|---|---|
| 0 | 810 | 640 | 750 | 795 | 695 | 570 | 8600 |
| 4 | 1030 | 630 | ---- | 885 | 770 | --- | 8650 |
| 8 | 1270 | 810 | 965 | 1110 | 890 | 995 | 8250 |
| 12 | 1240 | 1000 | ---- | 1030 | 945 | --- | 7900 |
| 16 | 810 | 670 | 1030 | 755 | 750 | 925 | 7650 |
| 20 | 585 | 510 | ---- | 585 | 530 | --- | 7300 |
| 24 | 460 | 312 | 412 | 452 | 460 | 515 | 6450 |
| 28 | 460 | 287 | ---- | 365 | 435 | --- | 5550 |
| 32 | 425 | 350 | 320 | 455 | 415 | 470 | 4800 |
| 36 | 412 | 350 | ---- | 365 | 425 | --- | 3950 |

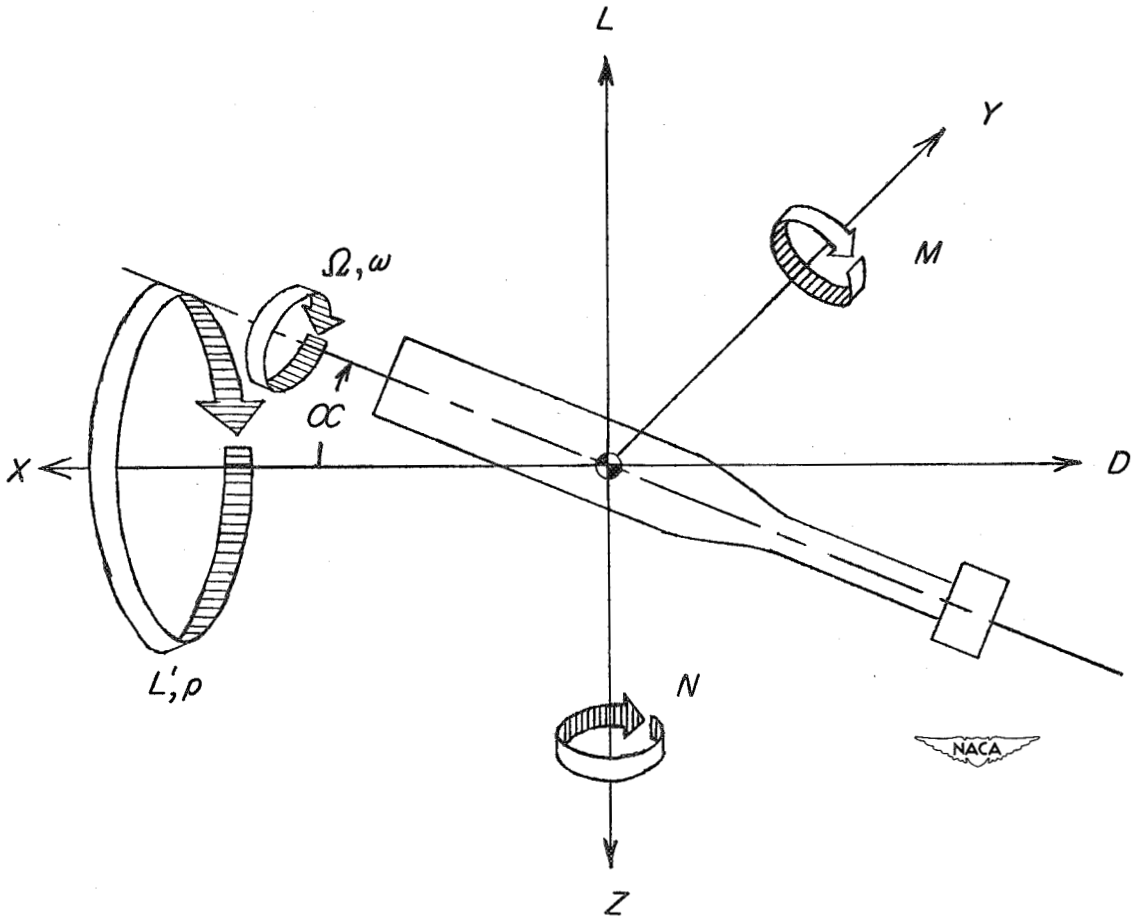


Figure 1.- System of axes used. Arrows indicate positive direction of forces, moments, angles, and angular velocities.

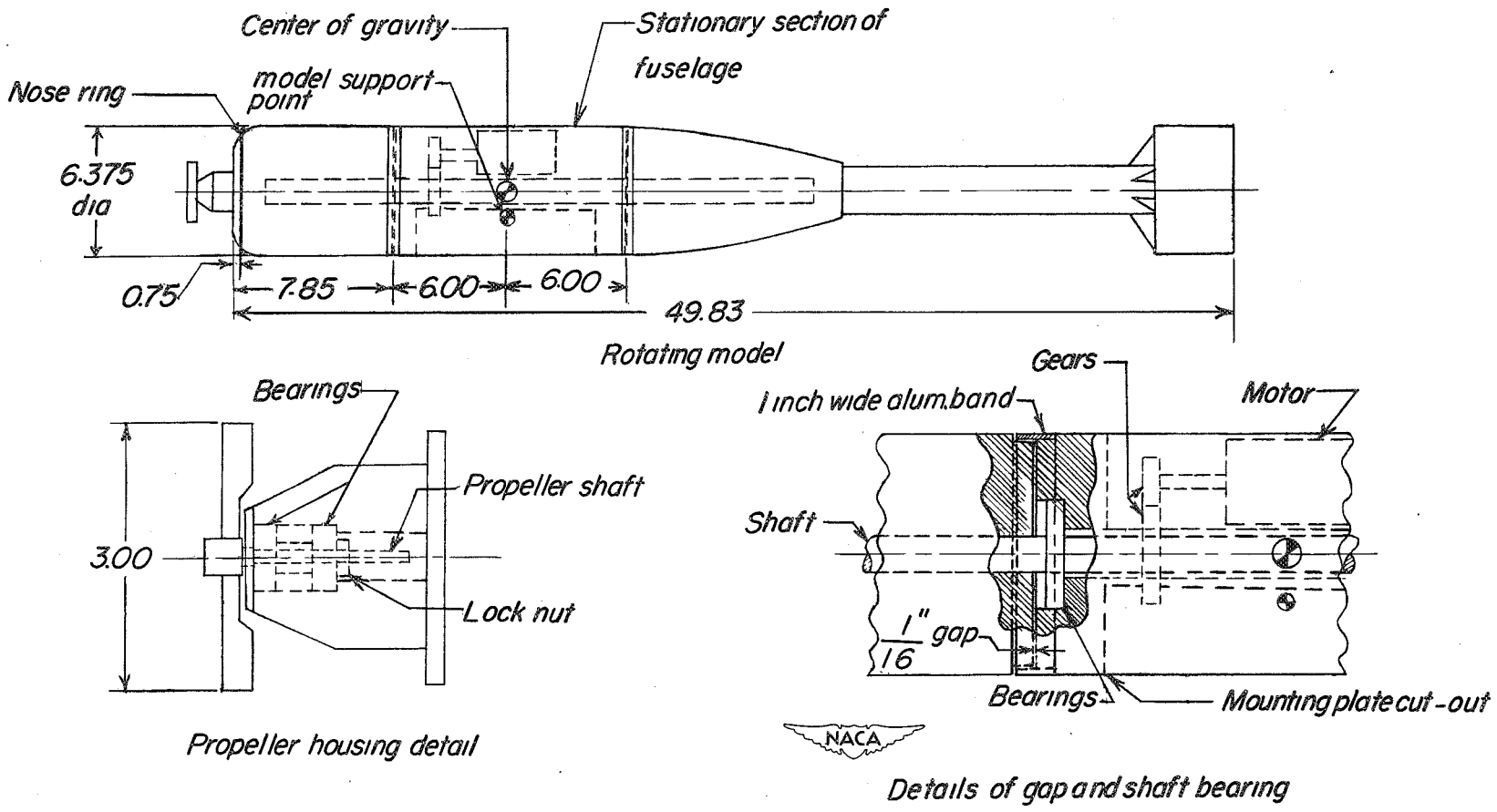


Figure 2.- Sketch of the rotating model. The stationary model had the same over-all dimensions except that it was one piece and the center of gravity and model support point coincided. All dimensions are in inches.

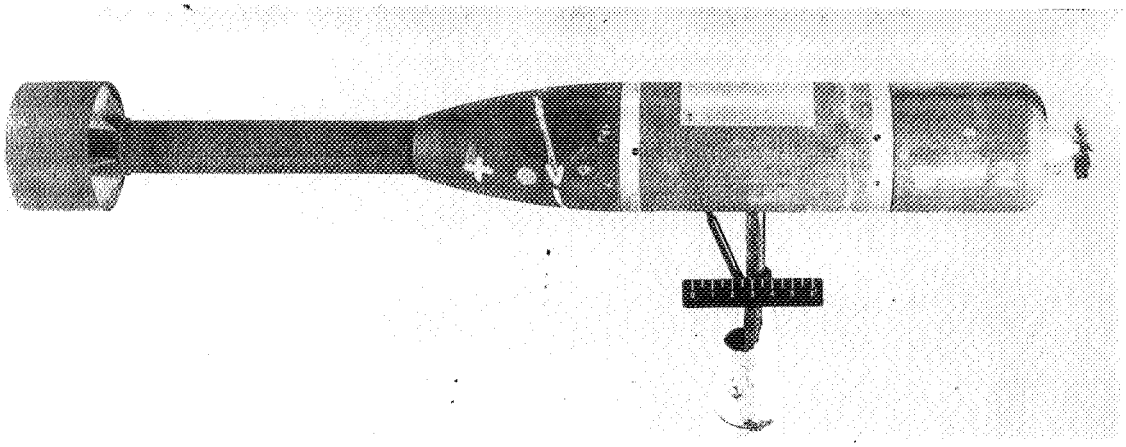

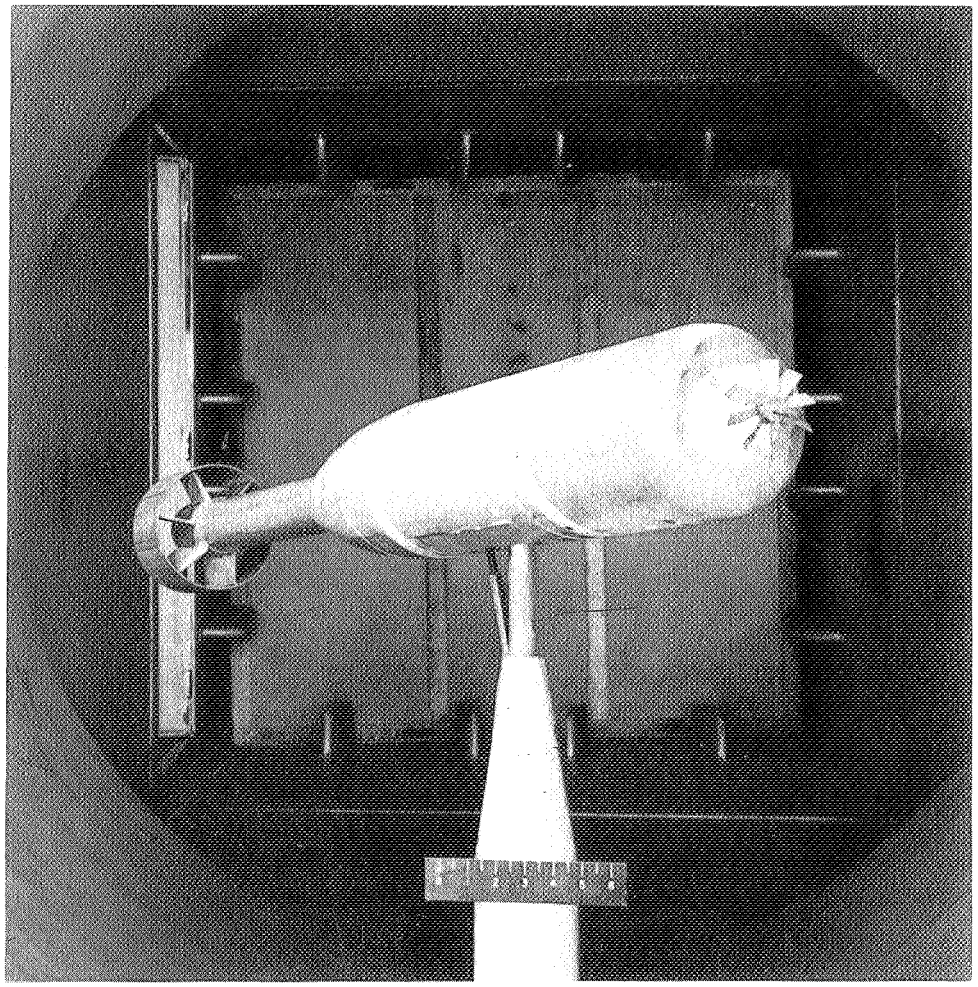

NACA

L-77017

Figure 3.- Photographs of the rotating model in the Langley stability tunnel.

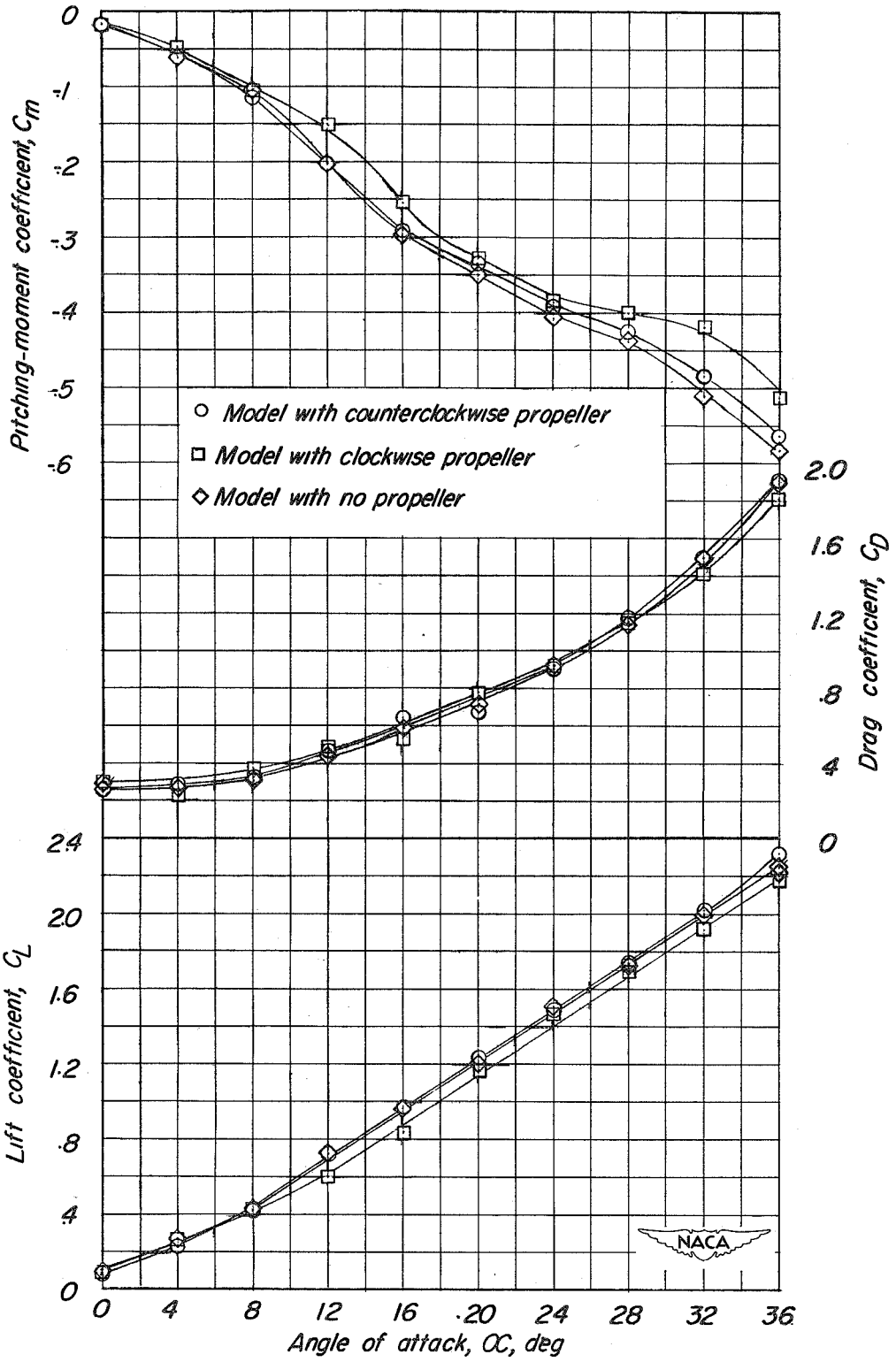


Figure 4.- Variation of aerodynamic coefficients with angle of attack for rotating model without nose ring.

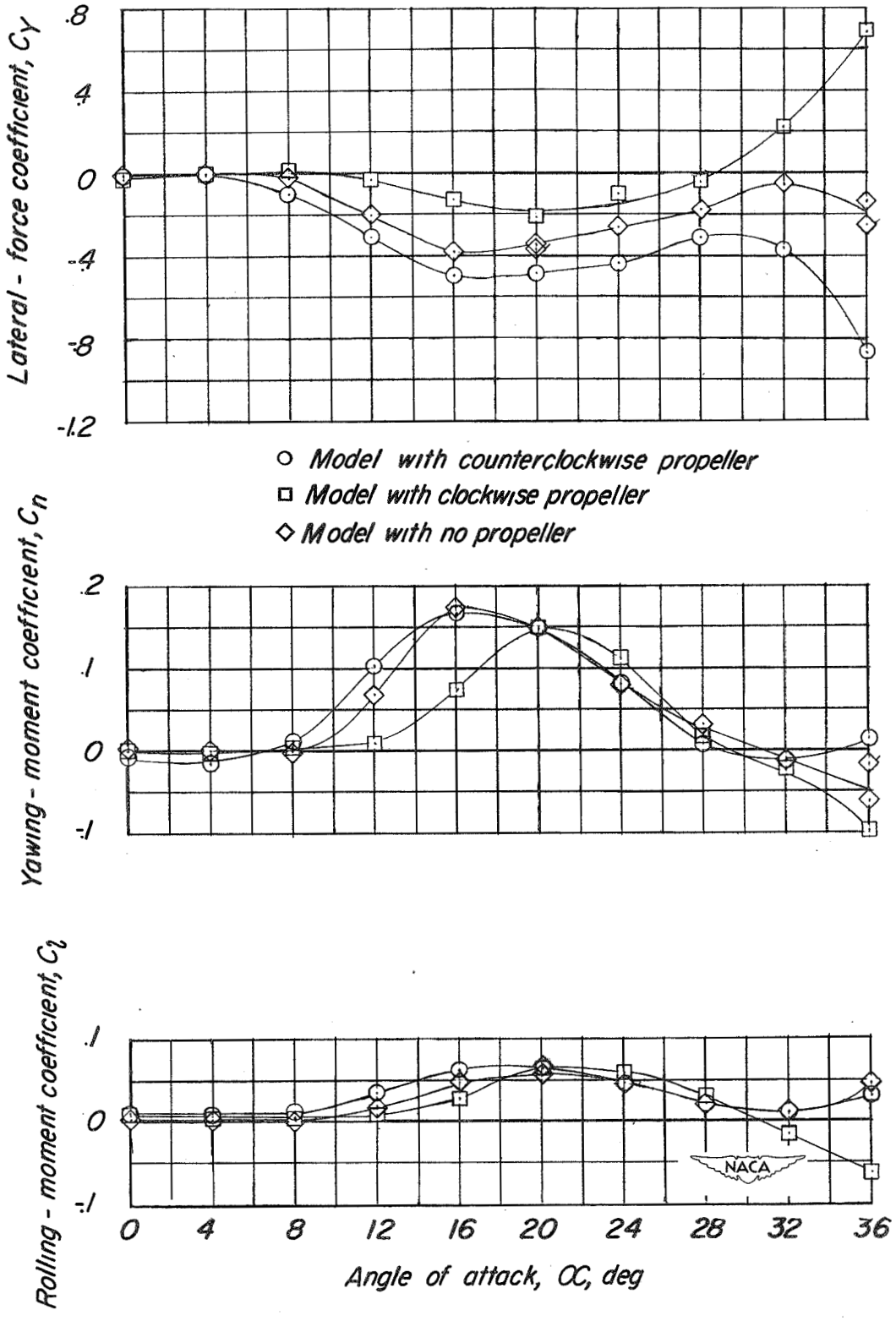


Figure 4.- Concluded.

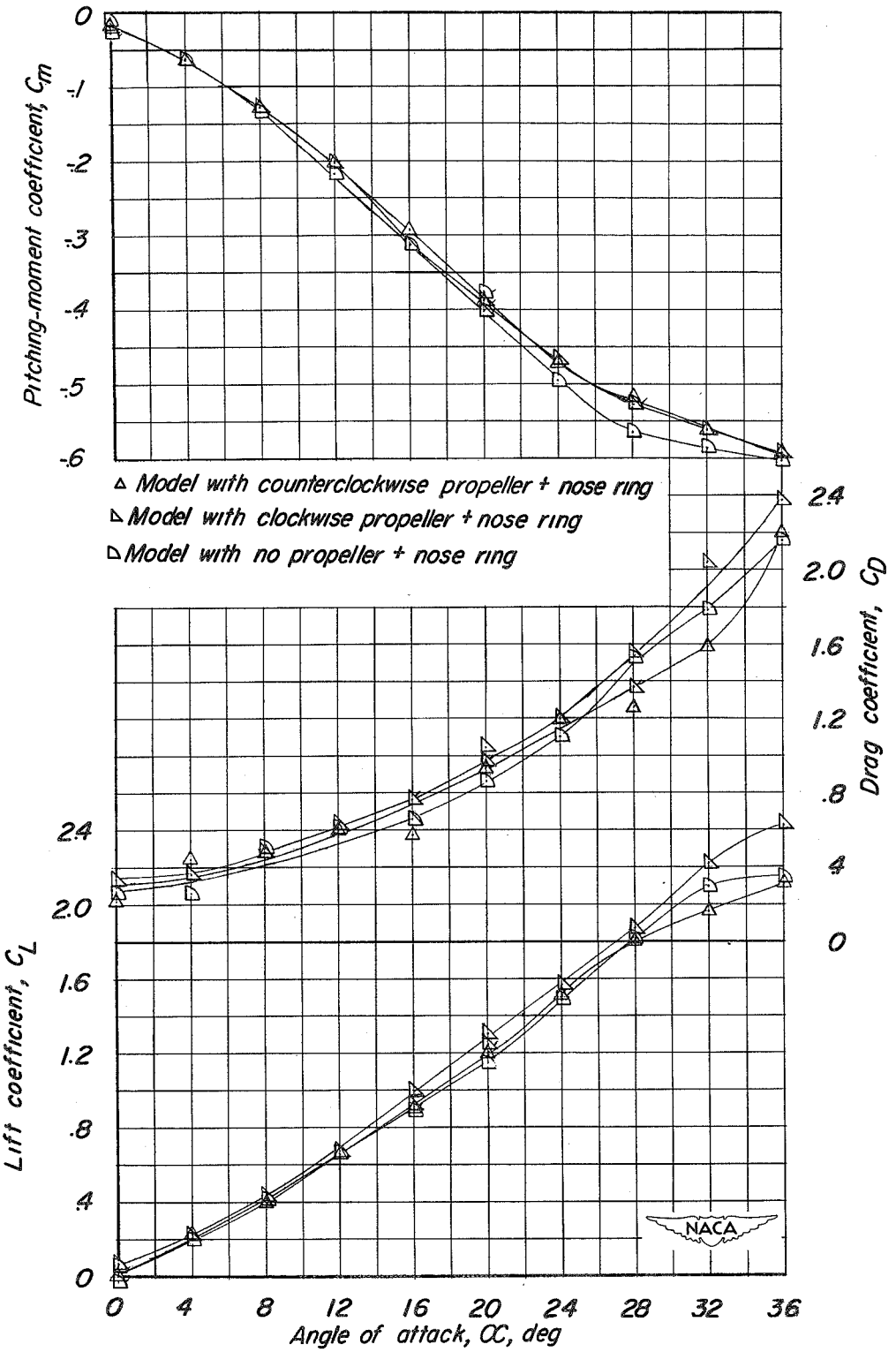


Figure 5.- Variation of aerodynamic coefficients with angle of attack for rotating model with nose ring.

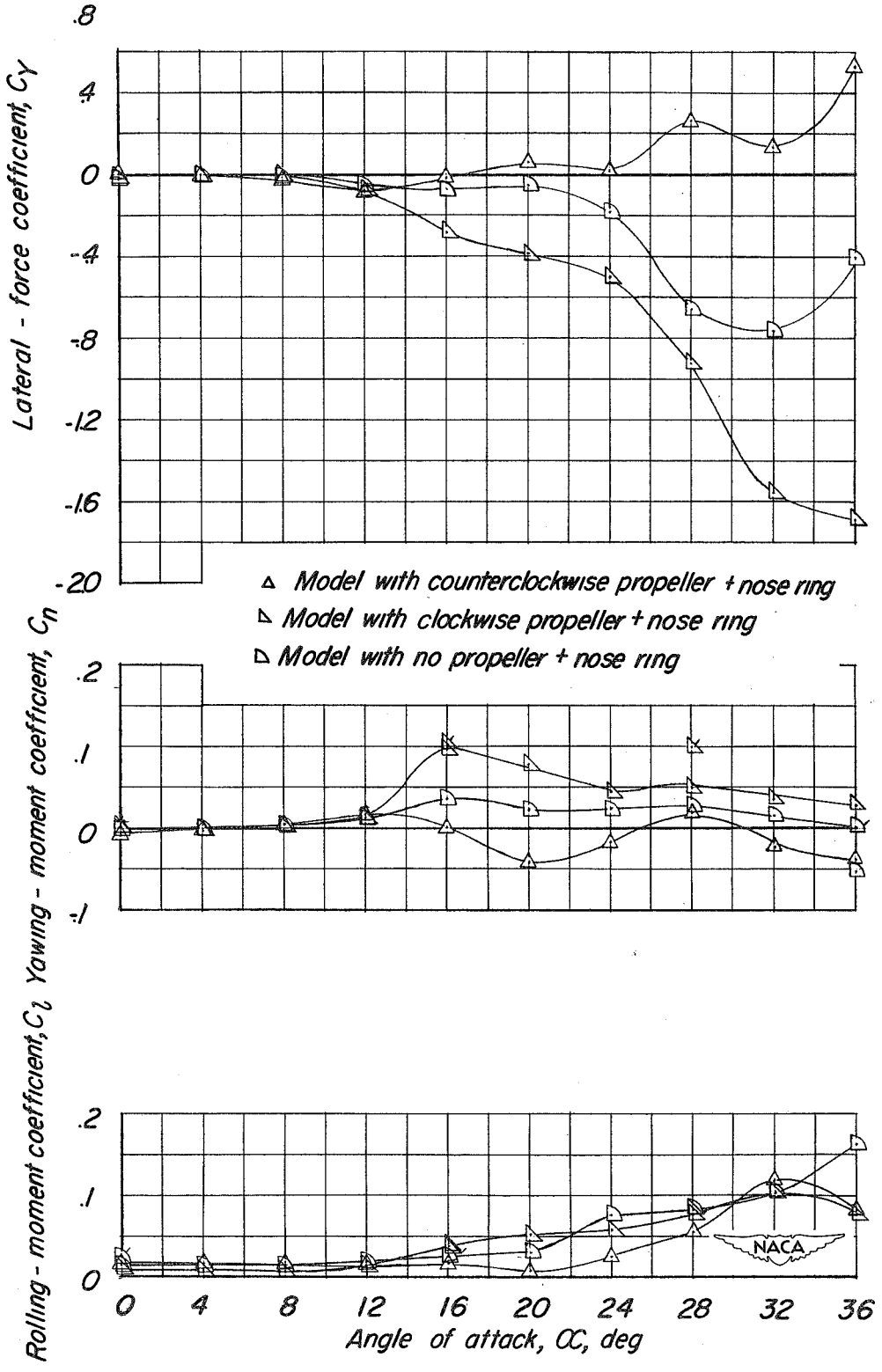


Figure 5.- Concluded.

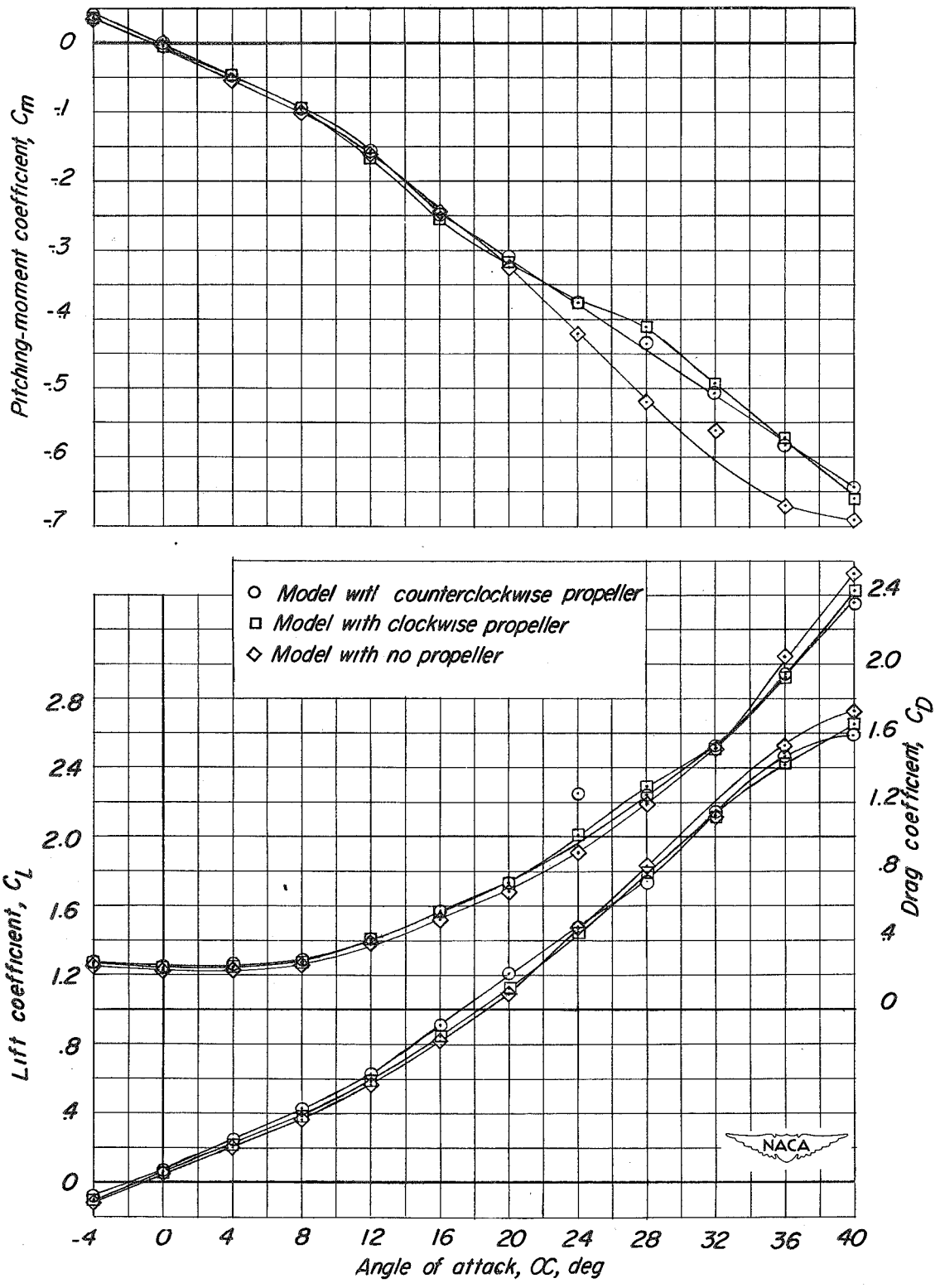


Figure 6.- Variation of aerodynamic coefficients with angle of attack for stationary model without nose ring.

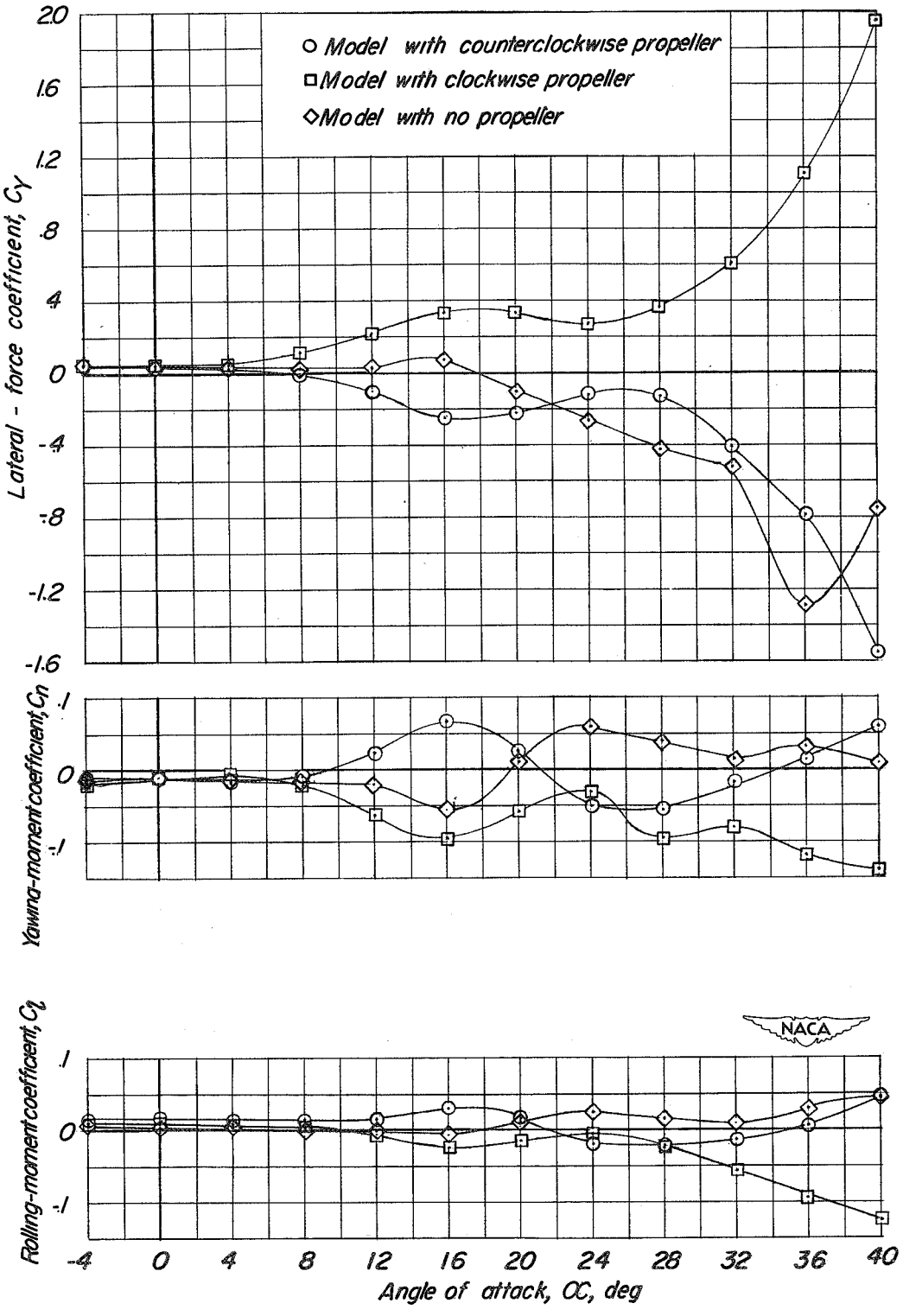


Figure 6.- Concluded.

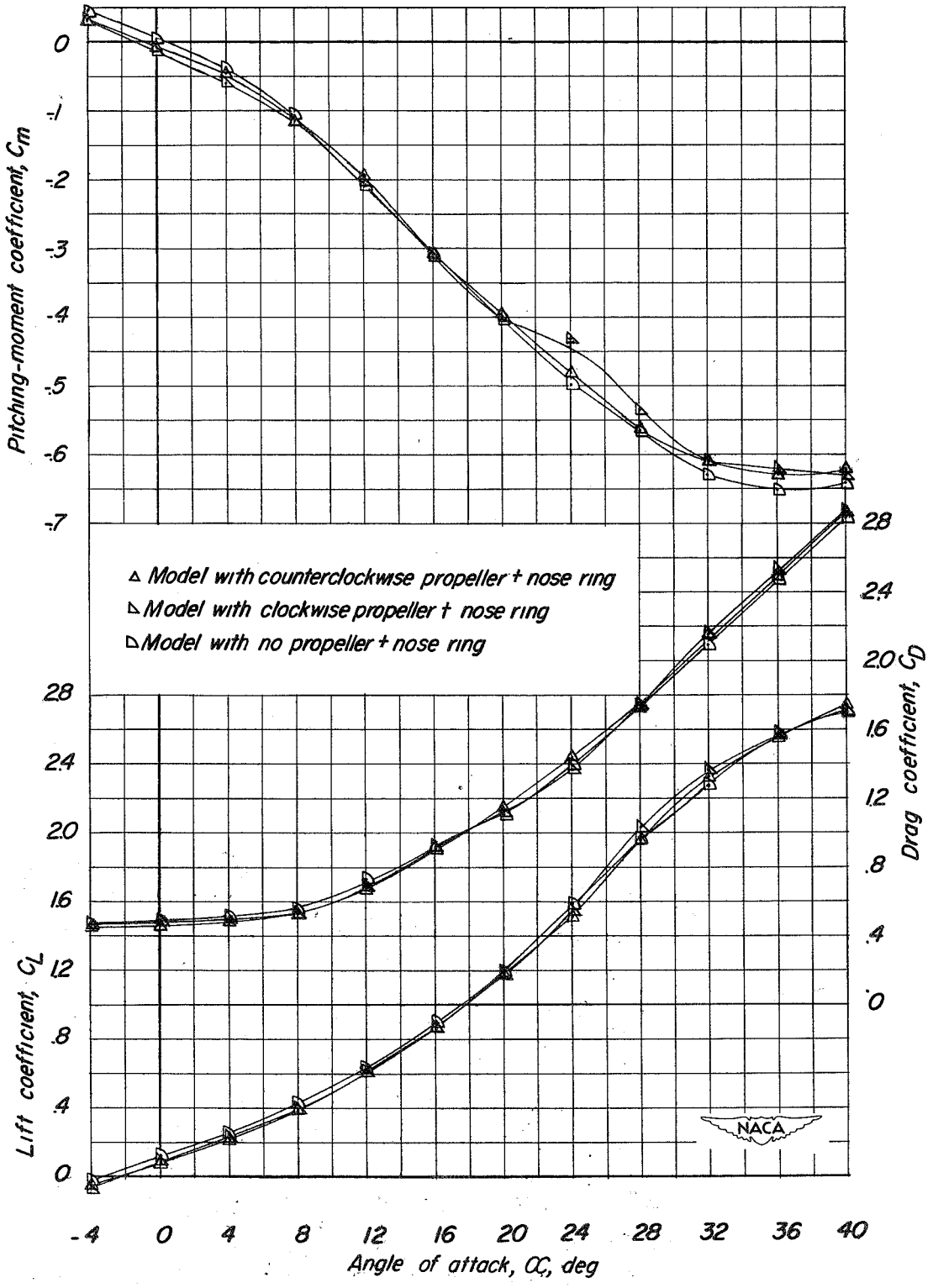


Figure 7.- Variation of aerodynamic coefficients with angle of attack for stationary model with nose ring.

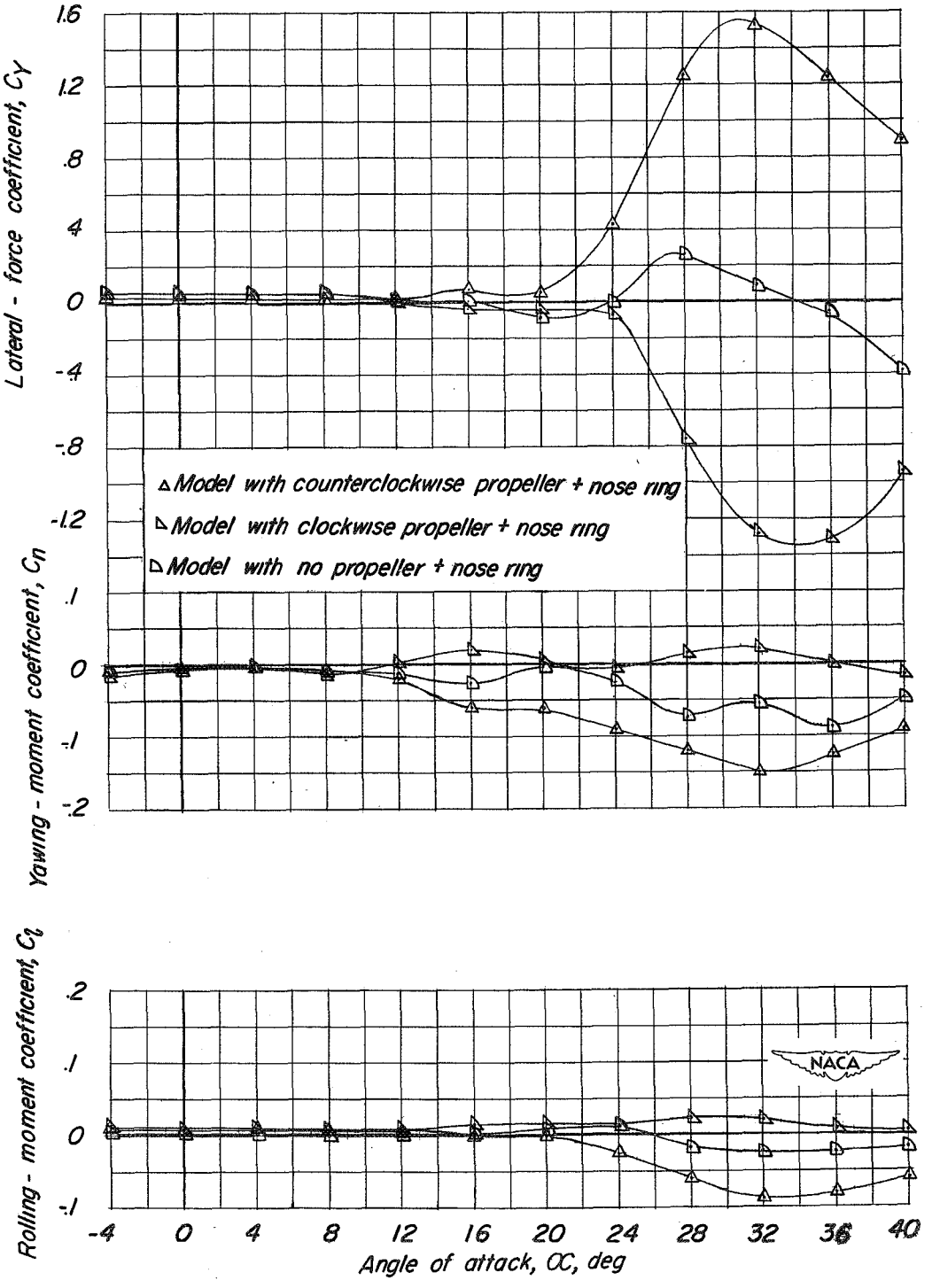


Figure 7.- Concluded.

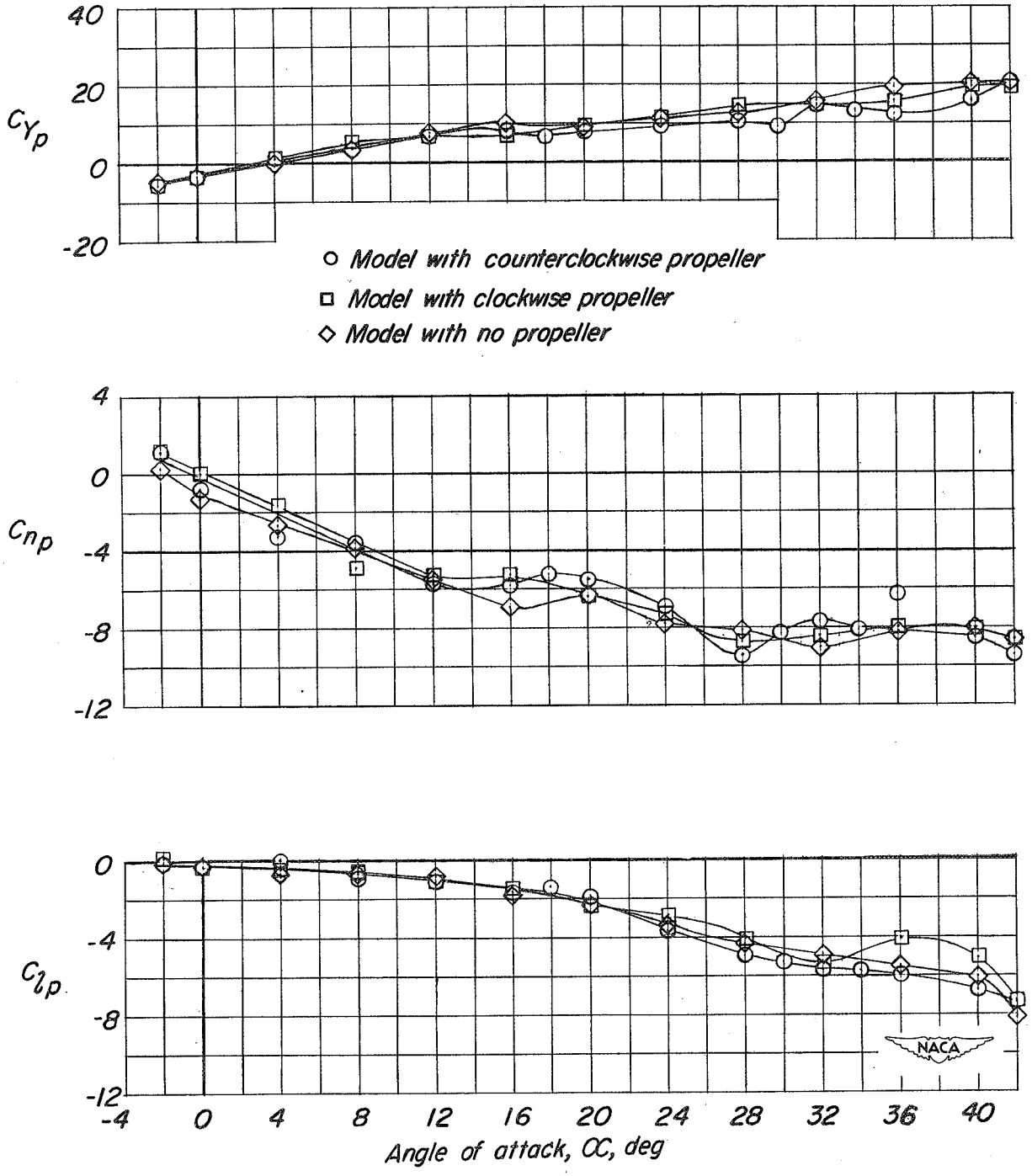


Figure 8.- Variation of rolling derivatives with angle of attack for rotating model without nose ring.

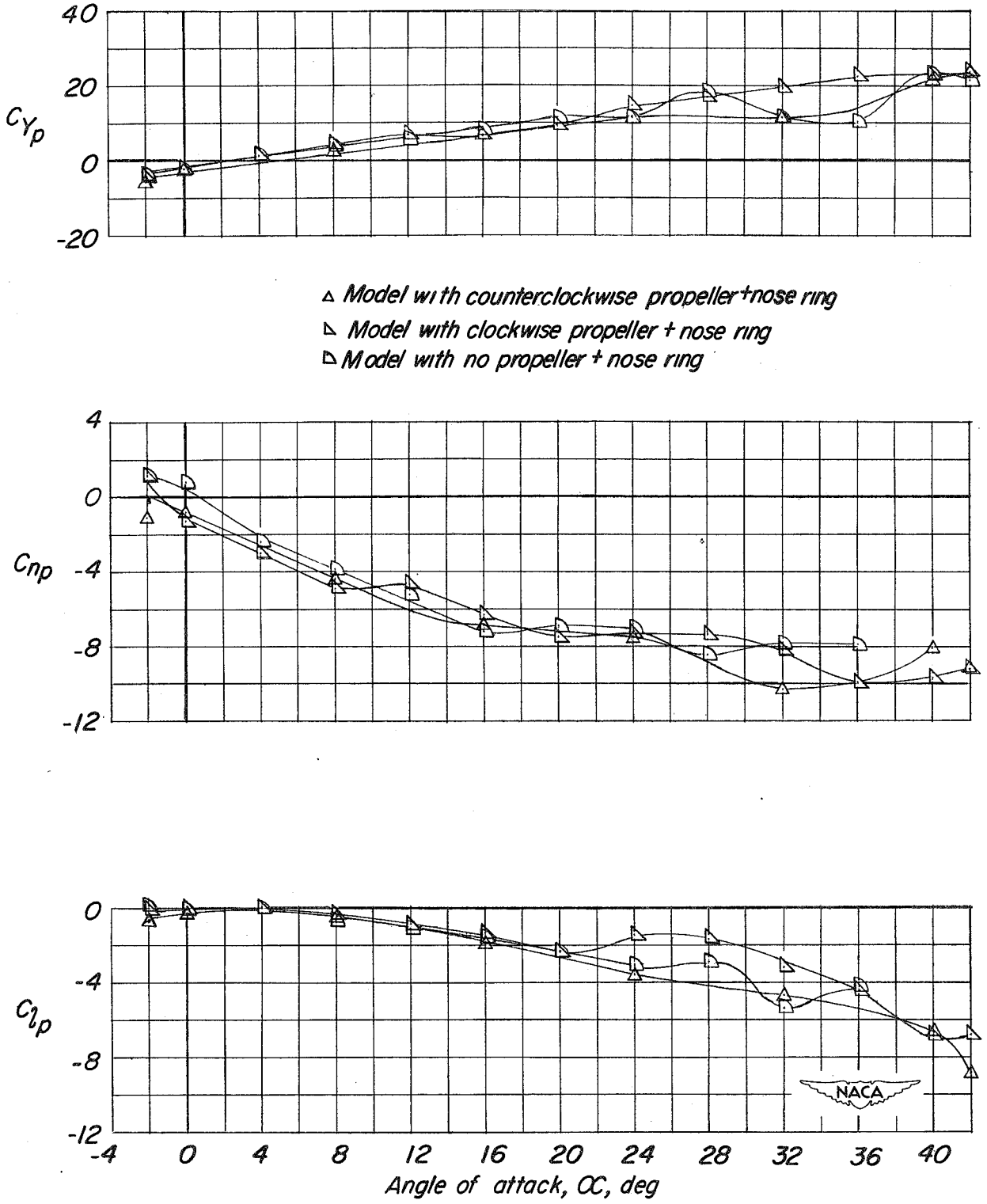


Figure 9.- Variation of rolling derivatives with angle of attack for rotating model with nose ring.

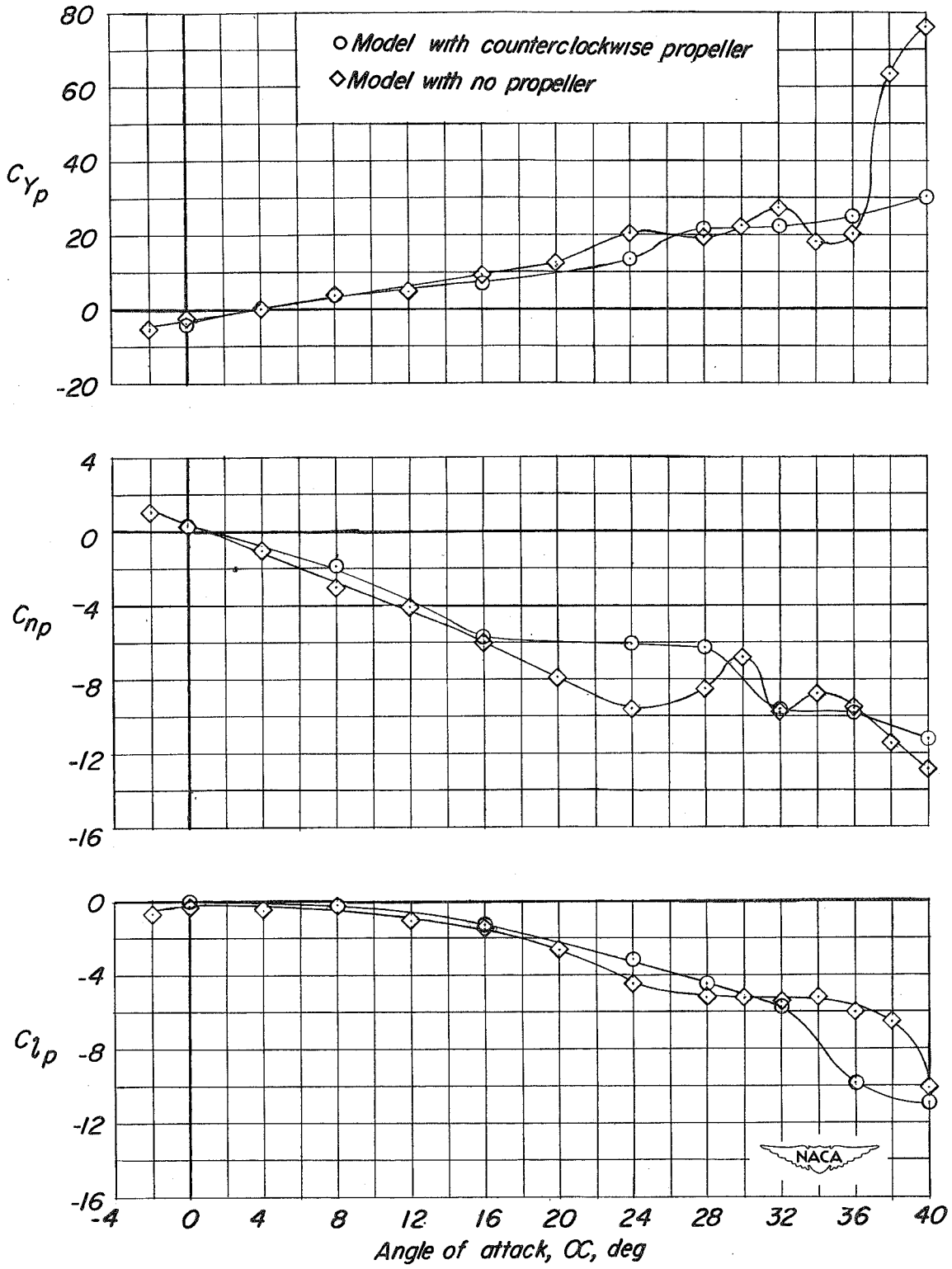


Figure 10.- Variation of rolling derivatives with angle of attack for stationary model without nose ring.

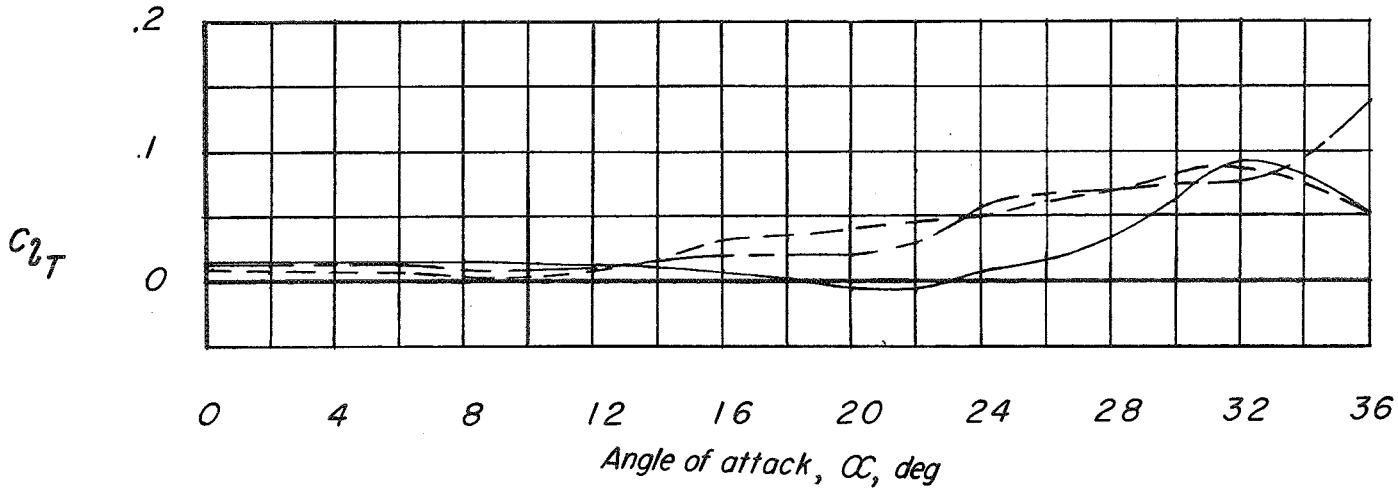


(a) Model with nose ring.

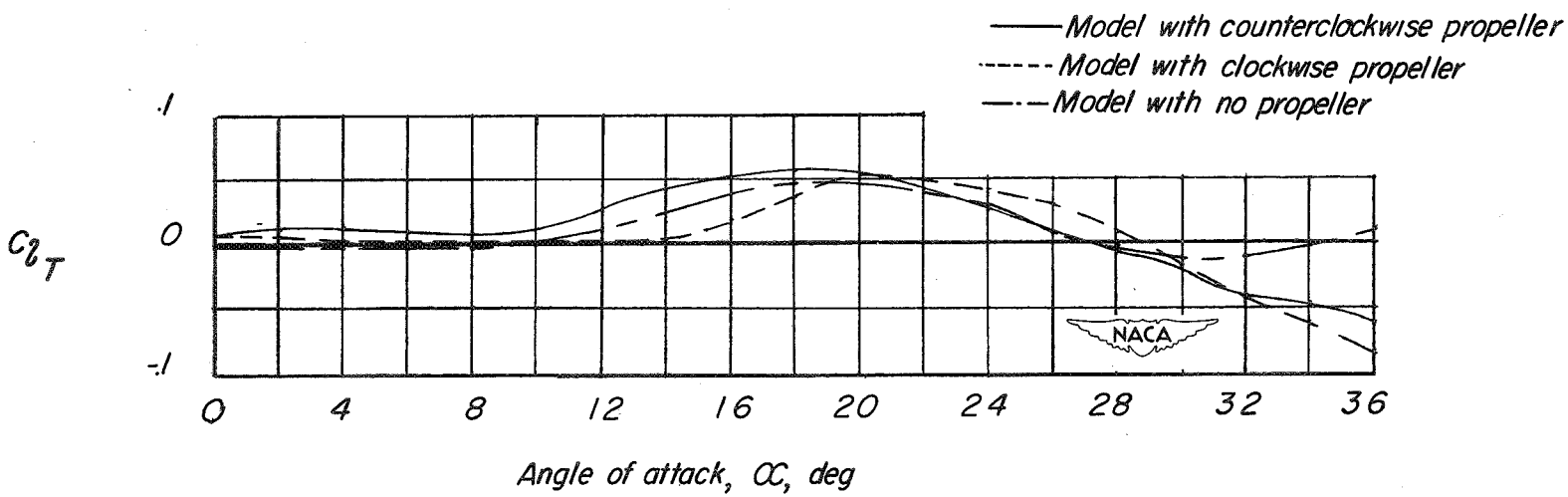


(b) Model without nose ring.

Figure 11.- Total rolling moment of spinning model.

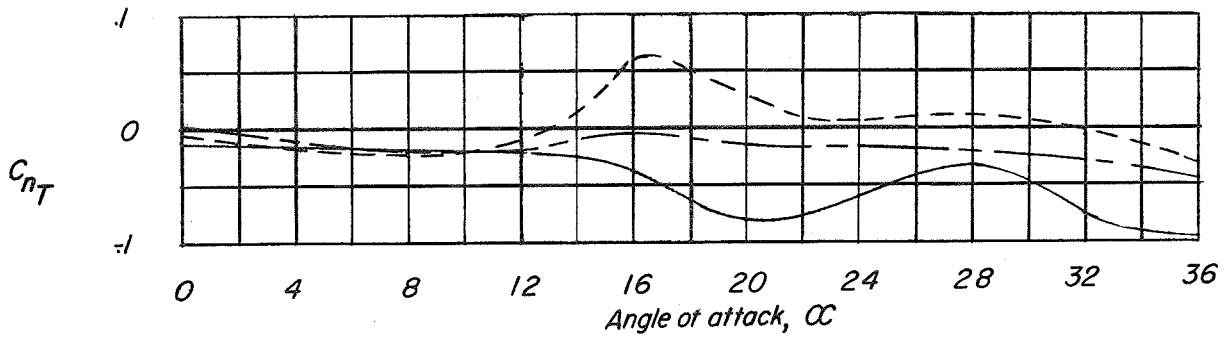


(a) Model with nose ring.

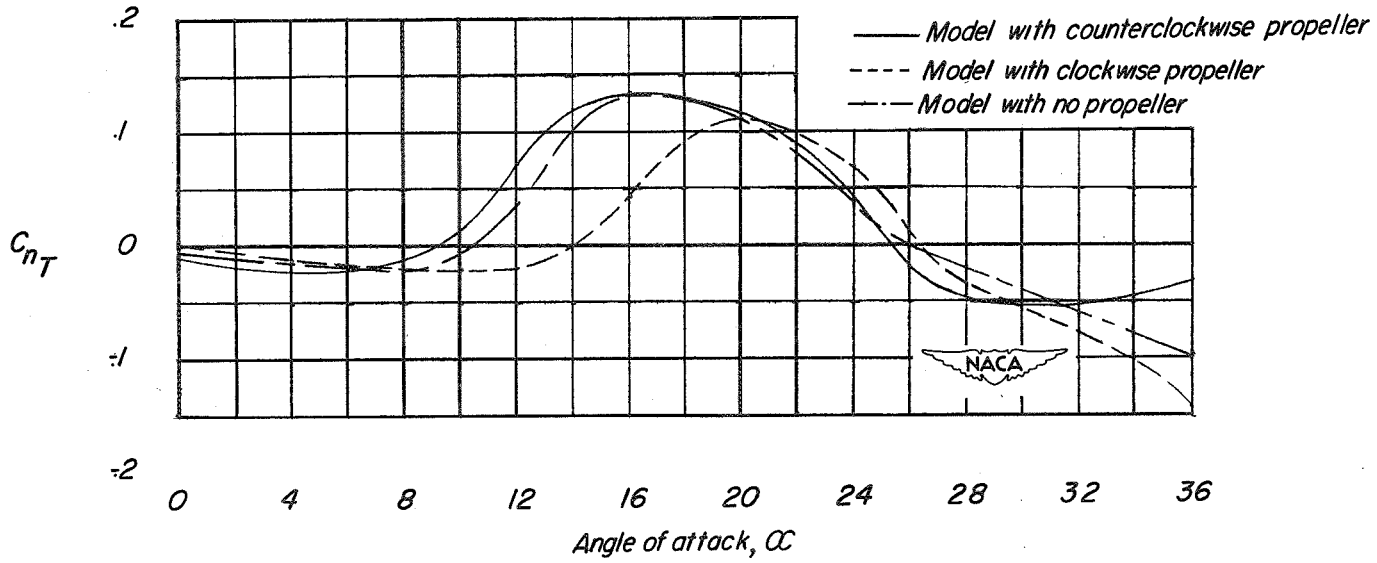


(b) Model without nose ring.

Figure 12.- Total yawing moment of spinning model.